

Alloy-fluctuation-induced exciton localization in high-Mg-content ($0.27 \leq x \leq 0.55$) wurtzite $\text{Mg}_x\text{Zn}_{1-x}\text{O}$ epilayers

This article has been downloaded from IOPscience. Please scroll down to see the full text article.

2010 J. Phys. D: Appl. Phys. 43 285402

(<http://iopscience.iop.org/0022-3727/43/28/285402>)

View [the table of contents for this issue](#), or go to the [journal homepage](#) for more

Download details:

IP Address: 159.226.35.185

The article was downloaded on 05/07/2010 at 02:09

Please note that [terms and conditions apply](#).

Alloy-fluctuation-induced exciton localization in high-Mg-content ($0.27 \leq x \leq 0.55$) wurtzite $\text{Mg}_x\text{Zn}_{1-x}\text{O}$ epilayers

Z L Liu¹, Z X Mei¹, R Wang¹, J M Zhao¹, H L Liang¹, Y Guo¹,
A Yu Kuznetsov² and X L Du^{1,3}

¹ Beijing National Laboratory for Condensed Matter Physics, Institute of Physics, Chinese Academy of Sciences, Beijing 100190, People's Republic of China

² Department of Physics, University of Oslo, PO Box 1048 Blindern, NO-0316 Oslo, Norway

E-mail: xldu@aphy.iphy.ac.cn

Received 9 March 2010, in final form 11 May 2010

Published 28 June 2010

Online at stacks.iop.org/JPhysD/43/285402

Abstract

Stokes shifts and near-band emission in high-Mg-content single-phase wurtzite $\text{Mg}_x\text{Zn}_{1-x}\text{O}$ ($0.27 \leq x \leq 0.55$) epilayers were investigated by photoluminescence (PL) and photoluminescence excitation combining laser and synchrotron excitation experiments. The observed Stokes shifts (e.g. 365 meV for the sample containing 55% Mg) as well as the 'S-shaped' temperature dependence of the maximum PL emissions were explained in terms of Mg compositional fluctuations in our sample resulting in exciton localization in potential traps and, consequently, suppression of non-radiative recombination making high-Mg-content MgZnO a good candidate for optical applications.

(Some figures in this article are in colour only in the electronic version)

In recent decades, wide band-gap semiconductor ZnO has been attracting intense attention particularly because of its interesting optoelectronic properties, e.g. significantly large exciton binding energy (60 meV) [1] compared with that of GaN (~26 meV). Moreover, by alloying ZnO with MgO, the band gap of MgZnO alloy can be tuned between that of wurtzite ZnO (~3.4 eV) and that of rock-salt MgO (~7.8 eV), which makes it a promising material for fabricating ultraviolet (UV) light emitting diodes [2, 3], UV detectors [4–6] and various heterostructures [7]. $\text{Mg}_x\text{Zn}_{1-x}\text{O}$ epitaxial layers were suggested to be efficient light emitters, even more efficient than ZnO, demonstrating remarkably enhanced photoluminescence (PL) correlated with the degree of exciton localization in low-Mg-content material ($x \leq 0.15$) [8]. Exciton localization caused by alloy compositional fluctuations has also been revealed by observation of large Stokes shift and S-shaped emission shifts in temperature-dependent PL measurements of wurtzite $\text{Mg}_x\text{Zn}_{1-x}\text{O}$ alloy having Mg contents in the range

$0 < x < 0.37$ [9]. It was suggested that the degree of localization will increase for higher Mg contents resulting in more efficient suppression of the non-radiative processes and consequently better optical performance. Addressing the challenge, a significant effort has been devoted to the synthesis of high-Mg-content wurtzite MgZnO alloys [10, 11] avoiding wurtzite-cubic phase separation and discovering reproducible synthesis routes. Very recently we have reported a realization of single-phase wurtzite $\text{Mg}_{0.55}\text{Zn}_{0.45}\text{O}$ films by employing an original quasi-homo buffer technique [12]. A photoconductive UV detector with a cutoff wavelength of 277 nm (well within the solar-blind range of the spectrum) was fabricated using a MgZnO film grown on a quasi-homo buffer [6]. At the present stage we see a need to document the fundamental optical properties of our material to gain a better understanding for correlating properties and device performance.

In this report, Stokes shifts and near-band emission in high-Mg-content single-phase wurtzite $\text{Mg}_x\text{Zn}_{1-x}\text{O}$ ($0.27 \leq x \leq 0.55$) epilayers were investigated by PL and

³ Author to whom any correspondence should be addressed.

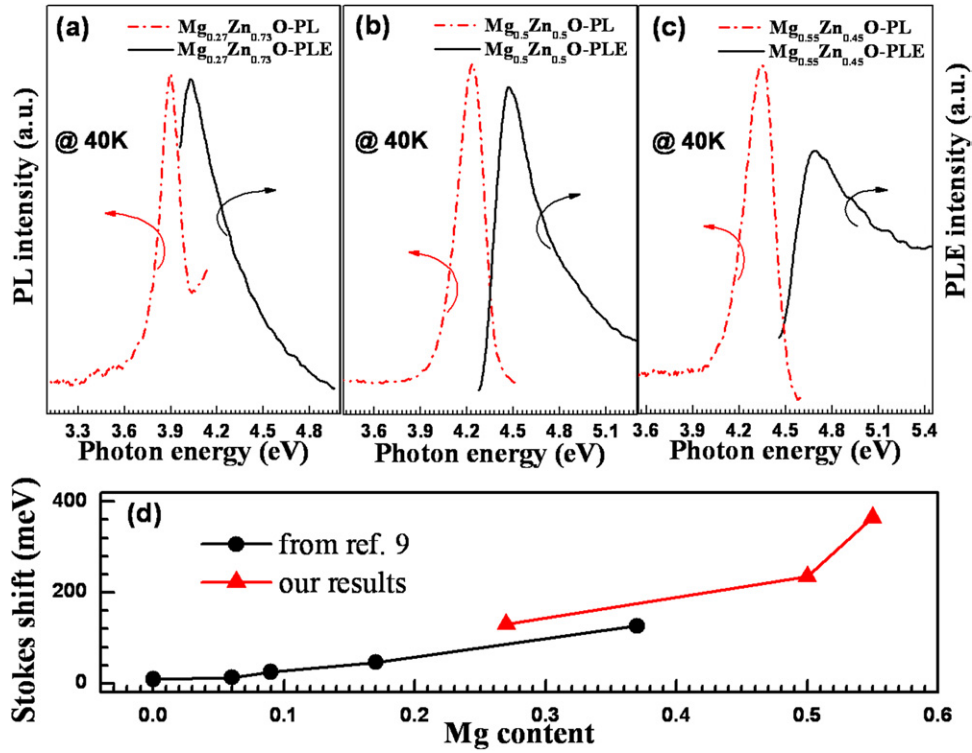


Figure 1. PL and PLE spectra as recorded at 40 K for (a) sample A (Mg_{0.27}Zn_{0.73}O), (b) sample B (Mg_{0.5}Zn_{0.5}O) and (c) sample C (Mg_{0.55}Zn_{0.45}O); and panel (d) summarizes the relationship between Stokes shifts (triangle spots) with Mg content (symbols—present work, line— [9]).

photoluminescence excitation (PLE) combining laser and synchrotron excitation experiments. MgZnO films were fabricated on sapphire (0001) substrates by rf-plasma assisted molecular beam epitaxy (rf-MBE) employing the quasi-homo buffer technique as required previously [12], and structural quality and composition were determined by x-ray diffraction and Rutherford back-scattering spectroscopy [12]. Among the host of samples, three samples were selected for this study, labelled sample A (Mg_{0.27}Zn_{0.73}O), sample B (Mg_{0.5}Zn_{0.5}O) and sample C (Mg_{0.55}Zn_{0.45}O). It should be noted that all the samples are obtained with a single wurtzite phase, so that no issues related to phase separation are to be taken into account when interpreting optical measurements. The temperature-dependent PL measurements were performed using 266 nm laser pulses at a repetition rate of 250 kHz and an average fluence of about 10 W cm⁻² (Coherence Inc.), and the spectrometer had a wavelength resolution of less than 0.09 nm. Low temperature (40 K) PL and PLE experiments were carried out using a synchrotron radiation UV light source (U24, National Synchrotron Radiation Laboratory) with a light flux of about 2 × 10⁹ photons s⁻¹ and a spot size of 0.3 × 3 mm². The whole light path was inside a high-vacuum chamber with a background pressure below 1 × 10⁻⁹ mbar, and the wavelength resolution was below 0.2 nm.

Figure 1 shows the 40 K PL and PLE spectra for samples A, B and C (see the respective panels) and the relationship between Stokes shifts and Mg contents (panel (d)). The wavelengths of the excitation light source for PL measurements of samples A, B and C were 290 nm, 266 nm and 260 nm, correlating with the band gaps in the samples. The PL peak

energies with maximum intensity in the near-band emission range (E_{PL}) were found to be 3.900 eV, 4.236 eV and 4.345 eV and full width at half maximum (FWHM) of PL emission peaks 162 meV, 198 meV and 214 meV, for samples A, B and C, respectively. Providing the corresponding Stokes shifts of 130 meV, 235 meV and 365 meV, the trend for the Stokes shifts to increase as a function of Mg content in MgZnO alloys is summarized in figure 1(d). It can be seen that the Stokes shift gradually increases consistently with the data in [9] and reaches a maximum value of 365 meV in the sample having 55% Mg. Stokes shift has been previously used in the literature to estimate the degree of alloy broadening effects and generation of localized tail states [9, 13]. Based on these terms the results in figure 1(d) suggest that the degree of localization in MgZnO increases as a function of Mg content interestingly. Compared with a similar effect in AlGaIn alloys [13], the compositional and band-gap fluctuations in MgZnO alloys may be more significant specifically judging from much larger Stokes shift values in high-Mg-content films (symbols in figure 1(d)).

The typical results of temperature-dependent PL measurements for samples A and C are shown in figure 2 and we emphasize the corresponding shift of E_{PL} positions in the samples. It is well established that E_{PL} values, in the first approximation, follow the temperature-dependent band-gap shrinking trend conventionally given by Varshni's equation, $E_g(T) = E_g(0) - \alpha T^2 / (\beta + T)$, where $E_g(T)$ and $E_g(0)$ are the band-gap transition energies at T and 0 K, respectively, while α and β are constants which we adapt for a further analysis from [14]: $\alpha = (8.2 \pm 0.3) \times 10^{-4}$ eV K⁻¹ and $\beta = (700 \pm 30)$ K as used for the A exciton transition

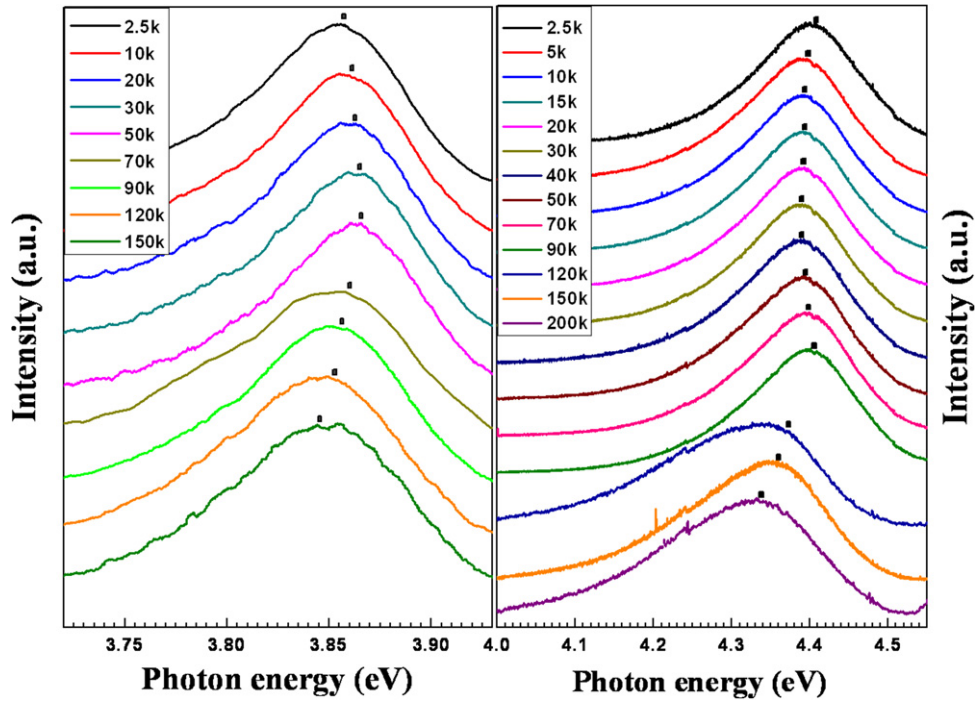


Figure 2. Temperature-dependent PL spectra of samples A ($\text{Mg}_{0.27}\text{Zn}_{0.73}\text{O}$) and C ($\text{Mg}_{0.55}\text{Zn}_{0.45}\text{O}$), as detected in the near-band emission range; symbols on top of the corresponding line label E_{PL} positions used in a further analysis.

of ZnO. In pure ZnO and MgZnO with a low Mg content, the evolution of E_{PL} with temperature normally follows the Varshni formalism resulting in a continuous red shift in the E_{PL} position [14]. However, figure 2 demonstrates a competing blue–red shift trend as well as a more complicated ‘S-shaped’ trend for samples A and C, respectively.

Note that the S-shaped temperature dependence of E_{PL} has been extensively investigated in (In,Al)GaN alloys exploiting these anomalous optical transitions in terms of the exciton localizations. A number of reports have shown that the excitons in InGaN are localized in deep traps within indium-rich regions resulting from partial phase segregation [15, 16], and it has a significant effect on the suppression of non-radiative processes and the performance of InGaN-based optical devices [17]. On the other hand, it was concluded that the exciton localization in AlGaIn originates from the alloy compositional fluctuations, since neither an ordering effect nor phase separation exists in these ternary alloys [13, 18, 19]. Similar to the case of AlGaIn, the x-ray diffraction results of our high-Mg-content MgZnO samples indicate the absence of ordered domains and phase mixing. Moreover, the FWHM values of (002) rocking curves for our $\text{Mg}_x\text{Zn}_{1-x}\text{O}$ ($x = 0.5$ and 0.55) samples decrease significantly from 0.06° and 0.23° (as-grown films) to 0.04° and 0.09° (after high-temperature annealing at 900°C), respectively, which indicates the thermal stability and high quality of these samples, as well as the single-phase structures. Based on this similarity we suggest that the excitons in our samples are localized in the band tail states generated by alloy compositional fluctuations, contributing to the S-shaped E_{PL} dependence in figure 2(b).

Figure 3 shows the band-gap shrinkage of ZnO plotted from Varshni’s formula (figure 3(a)) and the temperature dependence of PL peak energy for samples A and C

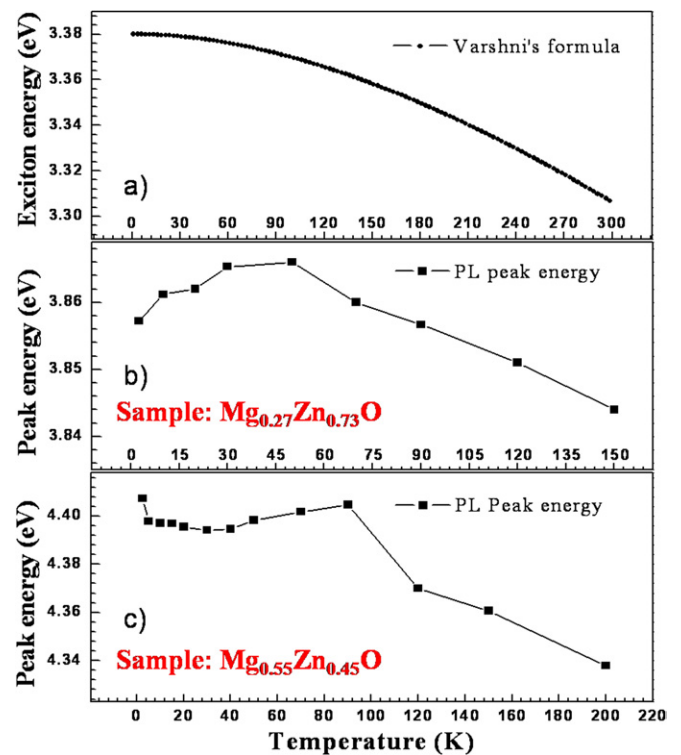


Figure 3. Temperature-dependent near-band-edge emission shift of (a) ZnO, (b) sample A ($\text{Mg}_{0.27}\text{Zn}_{0.73}\text{O}$) and (c) sample C ($\text{Mg}_{0.55}\text{Zn}_{0.45}\text{O}$).

(figures 3(b) and (c)), respectively. In the temperature range 2.5–50 K, a blue shift ($\sim 9\text{ meV}$) of the E_{PL} was observed for sample A ($\text{Mg}_{0.27}\text{Zn}_{0.73}\text{O}$). Taking into account the contribution of thermal band-gap shrinkage working towards red over this temperature range, the essential blue shift should

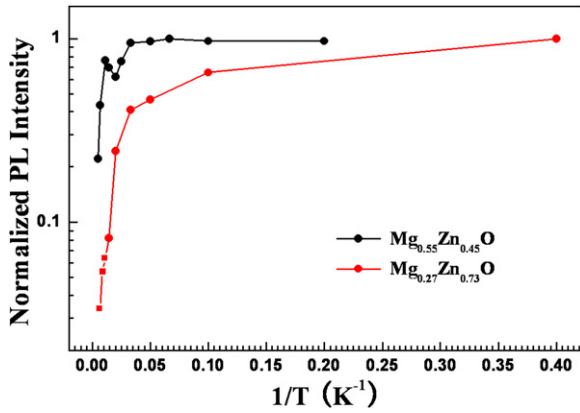


Figure 4. Arrhenius plots of normalized integrated PL intensities from sample A ($\text{Mg}_{0.27}\text{Zn}_{0.73}\text{O}$) and sample C ($\text{Mg}_{0.55}\text{Zn}_{0.45}\text{O}$).

be even larger. After 50 K, the E_{PL} is red shifted following the temperature dependence of the band gap shown in figure 3(b). As mentioned earlier the E_{PL} evolution in sample C is even more complicated (figure 3(c)). First from 2.5 to 30 K, E_{PL} shows a red-shift yielding ~ 13 meV, an order of magnitude higher than the normal energy shrinkage in accordance with Varshini (1 meV). When temperature increases from 30 to 90 K, E_{PL} increases gradually showing an anomalous blue-shift trend, while at temperatures >90 K E_{PL} follows the normal band-gap shrinkage. Such ‘S-shaped’ E_{PL} evolution in samples may be explained by the following mechanism. With the initial temperature increase, carriers localized in the lower potential minima will overcome the local potential barriers, occupy energetically deeper potential traps and recombine giving rise to a red shift of the luminescence energy. A further increase in the temperature will cause the thermal activation of the carriers relaxing their localization in the deepest potential minima, and thus results in a blue shift of E_{PL} . Finally, at higher temperatures the E_{PL} is determined by the normal temperature dependence of the band gap. In sample A having a significantly lower Mg content ($x = 0.27$), the degree of local potential fluctuations may be less pronounced, thus the first red-shift process cannot be distinguished in our measurements. The temperature for the blue-shift development increases with increasing Mg content from 50 K (sample A) to 90 K (sample C) indicating a higher thermal activation energy of the localized carriers in the deepest potential traps as well as bigger potential fluctuations, similar to the situation of the AlGaIn alloy [13].

In order to investigate the quantum efficiency (η) and carrier dynamics of PL emission from the localized excitons, the integrated PL intensity was analysed in the temperature range from 2.5 to 200 K and Arrhenius plots of the normalized integrated PL intensities are shown in figure 4. Assuming $\eta = 1$ at temperatures close to 0 K, the temperature-dependent lifetimes of radiation and non-radiation processes can be determined by the following formula: $I_{\text{PL}}(T)/I_{\text{PL}}(0\text{K}) \approx \eta(T) = \tau_{\text{total}}(T)/\tau_r(T) = 1 - 1/(1 + \tau_n(T)/\tau_r(T))$, where the total lifetime is determined by $1/\tau_{\text{total}} = 1/\tau_r + 1/\tau_n$, and τ_r and τ_n are the radiation and non-radiation lifetimes, respectively. At very low temperatures, the radiative processes dominate the recombination transitions. When the temperature increases to a critical point, the change from radiative to

non-radiative transition emerges, becoming dominant at higher temperatures. It can be found in figure 4 that the transition from radiative to non-radiative processes ($\tau_r = \tau_n$) occurs at about 20 K and 80 K for samples A ($\text{Mg}_{0.27}\text{Zn}_{0.73}\text{O}$) and C ($\text{Mg}_{0.55}\text{Zn}_{0.45}\text{O}$), respectively, correlating with thermal activation of localized carriers. Therefore, it can be concluded that the potential traps in MgZnO alloys are very efficient in inhibiting the non-radiative recombination and the phenomenon is more pronounced in MgZnO samples with a higher Mg content.

In summary, composition-fluctuation-induced exciton localization of high-Mg-content single-phase wurtzite MgZnO samples was investigated by low temperature PL and PLE and temperature-dependent PL. A large Stokes shift value (365 meV) indicates significant Mg compositional fluctuations in the $\text{Mg}_{0.55}\text{Zn}_{0.45}\text{O}$ alloy film. An anomalous ‘S-shaped’ temperature-dependent PL emission shift was observed, which is more pronounced in the higher Mg content samples. These phenomena are explained in terms of strong carrier localizations in potential traps suppressing non-radiative recombination processes, suggesting high-Mg-content MgZnO to be a promising material for optical electronics.

Acknowledgments

This work was supported by the National Science Foundation (Grant nos 50532090, 60606023, 60621091, 10804126, 10974246) and the Ministry of Science and Technology (Grant nos 2007CB936203, 2009CB929400) of China, partly supported by the National Synchrotron Radiation Laboratory, Hefei, China, as well as by the Research Council of Norway through the FRINAT ‘Understanding ZnO’ project.

References

- [1] Klingshirn C 1975 *Phys. Status Solidi* b **71** 547
- [2] Tang Z K, Wong G K L, Yu P, Kawasaki M, Ohtomo A, Koinuma H and Segawa Y 1998 *Appl. Phys. Lett.* **72** 3270
- [3] Ohtomo A, Kawasaki M, Ohkubo I, Koinuma H, Yasuda T and Segawa Y 1999 *Appl. Phys. Lett.* **75** 980
- [4] Zhang T C, Guo Y, Mei Z X, Gu C Z and Du X L 2009 *Appl. Phys. Lett.* **94** 113508
- [5] Yang W, Vispute R D, Choopun S, Sharma R P, Venkatesan T and Shen H 2001 *Appl. Phys. Lett.* **78** 2787
- [6] Du X L, Mei Z X, Liu Z L, Guo Y, Zhang T C, Hou Y N, Zhang Z, Xue Q K and Kuznetsov A Yu 2009 *Adv. Mater.* **21** 4625
- [7] Tsukazaki A, Ohtomo A, Kita T, Ohno Y, Ohno H and Kawasaki M 2007 *Science* **315** 1388
- [8] Shibata H, Tampo H, Matsubara K, Yamada A, Sakurai K, Ishizuka S, Niki S and Sakai M 2007 *Appl. Phys. Lett.* **90** 124104
- [9] Wassner T A, Laumer B, Maier S, Laufer A, Meyer B K, Stutzmann M and Eickhoff M 2009 *J. Appl. Phys.* **105** 023505
- [10] Ohtomo A, Kawasaki M, Koida T, Masubuchi K, Koinuma H, Sakurai Y, Yoshida Y, Yasuda T and Segawa Y 1998 *Appl. Phys. Lett.* **72** 2466
- [11] Takagi T, Tanaka H, Fujita S and Fujita S 2003 *Japan. J. Appl. Phys.* **42** L401

- [12] Liu Z L, Mei Z X, Zhang T C, Liu Y P, Guo Y, Du X L, Hallen A, Zhu J J and Kuznetsov A Yu 2009 *J. Cryst. Growth* **311** 4356–9
- [13] Cho Y, Gainer G H, Lam J B, Song J J, Yang W and Jhe W 2000 *Phys. Rev. B* **61** 7203
- [14] Wang L and Giles N C 2003 *J. Appl. Phys.* **94** 973
- [15] Martin R W, Middleton P G, O'Donnell K P and Van der Stricht W 1999 *Appl. Phys. Lett.* **74** 263
- [16] Zheng R and Taguchi T 2000 *Appl. Phys. Lett.* **77** 3024
- [17] Cho Y, Gainer G H, Fischer A J, Song J J, Keller S, Mishra U K and DenBaars S P 1998 *Appl. Phys. Lett.* **73** 1370
- [18] Chung S J, Kumar M S, Lee H J and Suh E K 2004 *J. Appl. Phys.* **95** 3565
- [19] Korakakis D, Ludwig K F Jr and Moustakas T D 1997 *Appl. Phys. Lett.* **71** 72